JCB Article

Runx2 induces osteoblast and chondrocyte differentiation and enhances their migration by coupling with PI3K-Akt signaling

Takashi Fujita,[1] Yasutaka Azuma,[2] Ryo Fukuyama,[3,4] Yuji Hattori,[1] Carolina Yoshida,[4,5] Masao Koida,[1] Kiyokazu Ogita,[1] and Toshihisa Komori[4]

[1]Department of Pharmacology, Faculty of Pharmaceutical Sciences, Setsunan University, Hirakata 573-0101, Japan
[2]Department of Pharmacology, Osaka Dental University, Hirakata 573-1121, Japan
[3]Laboratory of Pharmacology, Faculty of Pharmaceutical Sciences, Hiroshima International University, Kure 737-0112, Japan
[4]Division of Oral Cytology and Cell Biology, Department of Developmental and Reconstructive Medicine, Nagasaki University Graduate School of Biomedical Sciences, Nagasaki 852-8588, Japan
[5]Department of Orthodontics and Dentofacial Orthopedics, Osaka University Faculty of Dentistry, Suita, Osaka 565-0871, Japan

Runx2 and phosphatidylinositol 3-kinase (PI3K)–Akt signaling play important roles in osteoblast and chondrocyte differentiation. We investigated the relationship between Runx2 and PI3K-Akt signaling. Forced expression of *Runx2* enhanced osteoblastic differentiation of C3H10T1/2 and MC3T3-E1 cells and enhanced chondrogenic differentiation of ATDC5 cells, whereas these effects were blocked by treatment with IGF-I antibody or LY294002 or adenoviral introduction of dominant-negative (dn)–*Akt*. Forced expression of *Runx2* or dn-*Runx2* enhanced or inhibited cell migration, respectively, whereas the enhancement by Runx2 was abolished by treatment with LY294002 or adenoviral introduction of dn-*Akt*. Runx2 up-regulated PI3K subunits (p85 and p110β) and Akt, and their expression patterns were similar to that of Runx2 in growth plates. Treatment with LY294002 or introduction of dn-*Akt* severely diminished DNA binding of Runx2 and Runx2-dependent transcription, whereas forced expression of myr*Akt* enhanced them. These findings demonstrate that Runx2 and PI3K-Akt signaling are mutually dependent on each other in the regulation of osteoblast and chondrocyte differentiation and their migration.

Introduction

The formation of bone structures in vertebrates involves osteoblast and chondrocyte differentiation. Osteoblast and chondrocyte differentiation are regulated by many secreted differentiation factors including TGFβs, bone morphogenetic proteins, insulin-like growth factors (IGFs), FGFs, parathyroid hormone (PTH), PTH–related peptide, thyroid hormone, Indian hedgehog, and retinoic acid (Karaplis, 2002). Furthermore, transcription factors play fundamental roles in osteoblast and chondrocyte differentiation. Runx2 (runt-related transcription factor 2)/Cbfa1 (core binding factor α1)/Pebp2αA (polyoma enhancer binding protein 2αA) and Osterix are essential for osteoblast differentiation (Komori et al., 1997, Otto et al., 1997, Nakashima et al., 2002); Sox5, Sox6, and Sox9 are essential for chondrocyte differentiation (Bi et al., 1999, Smits et al., 2001); and Runx2 plays an important role in terminal chondrocyte differentiation (Enomoto et al., 2000, Ueta et al., 2001).

Runx2 is a transcription factor that belongs to the Runx family (Komori 2002). *Runx2*-deficient (*Runx2*$^{-/-}$) mice completely lack bone formation owing to the absence of osteoblasts (Komori et al., 1997, Otto et al., 1997). Runx2 determines the osteoblast lineage from multipotent mesenchymal cells, induces osteoblastic differentiation at the early stage, and inhibits it at the late stage (Liu et al., 2001, Komori 2002). Further, Runx2 has been shown to induce alkaline phosphatase (ALP) activity, expression of bone matrix protein genes, and mineralization in immature mesenchymal cells and osteoblastic cells in vitro (Banerjee et al., 1997, Ducy et al., 1997, Harada et al., 1999). Chondrocyte differentiation is also disturbed in *Runx2*$^{-/-}$ mice (Inada et al., 1999, Kim et al., 1999). Overexpression of *Runx2* or the

Address correspondence to T. Komori, Division of Oral Cytology and Cell Biology, Dept. of Developmental and Reconstructive Medicine, Nagasaki University Graduate School of Biomedical Sciences, 1-7-1 Sakamoto, Nagasaki 852-8588, Japan. Tel.: 81-95-849-7630. Fax: 81-95-849-7633. email: komorit@net.nagasaki-u.ac.jp

Key words: Cbfa1; IGF; MEK; myrAkt; chemotaxis

dominant-negative (dn) form of *Runx2* (dn-*Runx2*) in chondrocytes accelerates or decelerates chondrocyte maturation, respectively, indicating that Runx2 is a positive regulatory factor in chondrocyte maturation (Ueta et al., 2001). Further, introduction of dn-*Runx2* inhibited cell condensation in insulin-induced chondrogenesis of ATDC5 cells (Akiyama et al., 1999). Thus, Runx2 plays crucial roles in osteoblast and chondrocyte differentiation (Komori 2002).

Mutant mice that lack both *Igf1* and *Igf2* and mice that lack the *Igf1r* show severe retardation of bone development, and both *Irs1*-deficient mice and *Irs2*-deficient mice show an osteopenic phenotype (Liu et al., 1993, Ogata et al., 2000, Akune et al., 2002). Therefore, IGFs and their signaling molecules play important roles in skeletal development by regulating osteoblast and chondrocyte differentiation. Akt is a serine-threonine kinase whose amino terminus contains a pleckstrin homology, and is activated by various extracellular stimuli including insulin and IGF through the phosphatidylinositol 3-kinase (PI3K) pathway (Scheid and Woodgett, 2001). In various cell culture systems, PI3K-Akt signaling has been implicated as a critical pathway for the differentiation of skeletal component cells including chondrocytes, osteoblasts, myoblasts, and adipocytes (Kaliman et al., 1996, Sakaue et al., 1998, Hidaka et al., 2001, Ghosh-Choudhury et al., 2002). Further, bone development is severely delayed in mice lacking both *Akt1* and *Akt2* (Peng et al., 2003). However, the mechanism of the differentiation of skeletal component cells mediated by PI3K-Akt signaling remains to be clarified.

PDGF, IGF, and VEGF work as chemotactic factors through PI3K, and PI3K-Akt signaling is a major pathway for chemotaxis through G-protein–coupled receptors in *Dictyostelium discoideum* and in neutrophils and through tyrosine kinase receptors in fibroblasts. After activation of PI3K at the leading edge, Akt rapidly accumulates by binding to PtdIns(3,4,5)P_3 via its pleckstrin homology domain, leading to activation of Akt by phosphorylation. Akt likely mediates cell migration at least partly by activating Rac and p21-activated protein kinase (Ridley et al., 2003).

Although Runx2 is an important transcription factor for osteoblast and chondrocyte differentiation, and PI3K-Akt signaling is deeply involved in the differentiation of skeletal component cells, the relationship between Runx2 and PI3K-Akt signaling is not known. In this study, we investigated the involvement of PI3K-Akt signaling in the function of Runx2 using immature mesenchymal C3H10T1/2 cells, immature osteoblastic MC3T3-E1 cells, and prechondrogenic ATDC5 cells, and found that Runx2 induces osteoblast and chondrocyte differentiation and enhances their migration by coupling with PI3K-Akt signaling.

Results

PI3K-Akt signaling is involved in Runx2-dependent osteoblast differentiation

To elucidate if PI3K-Akt signaling is involved in Runx2-dependent osteoblast and chondrocyte differentiation, we established *Runx2* or dn-*Runx2* stable transfectants from an immature osteoblastic cell line, MC3T3-E1, an immature mesenchymal cell line, C3H10T1/2, and an insulin-dependent prechondrogenic cell line, ATDC5 (Fig. 1, A and B). The differentiation of MC3T3-E1 cells was enhanced in *Runx2* stable transfectants but inhibited in dn-*Runx2* stable transfectants in comparison with that in the wild-type MC3T3-E1 cells, as indicated by the levels of ALP activity and calcium deposition (Fig. 2, A and B). MC3T3-E1 cells secrete IGF-I (Huang et al., 2000). The Runx2-induced enhancement of ALP activity and mineralization was blocked by treatment with either a neutralizing antibody against IGF-I or a PI3K inhibitor, LY294002, in a dose-dependent manner (Fig. 2 C), indicating that IGF-I receptor-PI3K signaling is required for Runx2 activity in MC3T3-E1 cells. Further, adenoviral introduction of dn-*Akt* blocked Runx2-induced ALP activity and mineralization (Fig. 2 D). ALP activity was also induced in *Runx2* stable transfectants from C3H10T1/2 cells, whereas it was abrogated by adenoviral introduction of dn-*Akt* (Fig. 2 E). These findings indicate that PI3K-Akt signaling is involved in Runx2-dependent osteoblast differentiation.

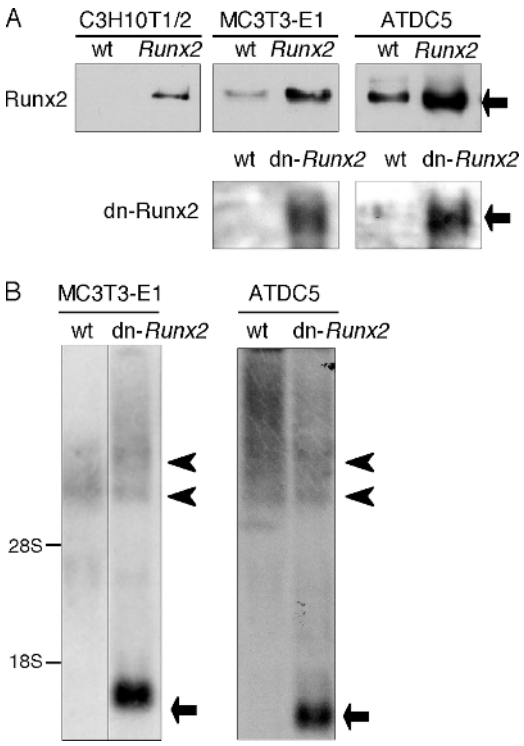

Figure 1. **Establishment of *Runx2* or dn-*Runx2* stable transfectants.** *Runx2* or dn-*Runx2* stable transfectants were established from C3H10T1/2, MC3T3-E1, and ATDC5 cells as described in Materials and methods. The expression level of Runx2 was examined by Western blot analysis (A) and that of dn-*Runx2* was examined by Western blot (A) and Northern blot (B) analyses. (A) The arrows show the bands for endogenous and exogenous Runx2 protein expression or exogenous dn-Runx2 protein expression. (B) Arrows show the bands for exogenous dn-*Runx2* mRNA. Arrowheads show the bands for endogenous *Runx2* mRNA. White lines indicate that intervening lanes have been spliced out. wt, wild-type cells. Representative data from four to five independent clones are shown. Dn-Runx2 protein was detected using an anti-Runx2 antibody, which specifically recognizes the NH_2 terminus of Runx2.

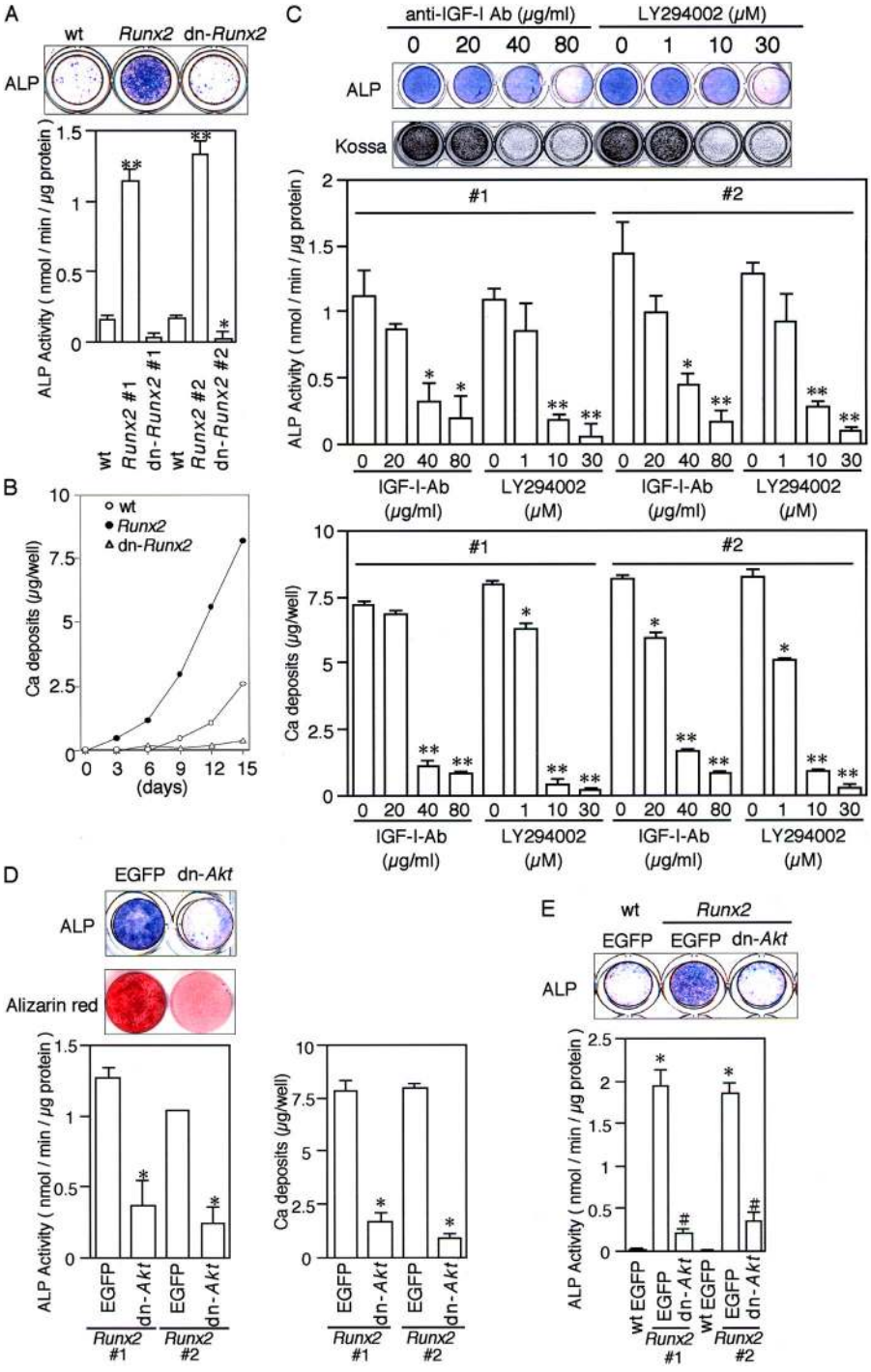

Figure 2. **Blockage of PI3K-Akt signaling inhibits Runx2-dependent osteoblast differentiation .** After confluence, wild-type cells and *Runx2* or dn-*Runx2* stable transfectants of MC3T3-E1 cells (A–D) and C3H10T1/2 cells (E) were cultured with 50 μg/ml ascorbic acid and 10 mM β-glycerophosphate and were examined for ALP activity after culture for 3 d and for mineralization after culture for 7 d. ALP activity (A) and the calcium content (B) in wild-type MC3T3-E1 cells (wt) and *Runx2* or dn-*Runx2* stably transfected MC3T3-E1 cells. ALP activities in two independent clones (#1 and #2) are presented as mean ± SEM of six wells. *, $P < 0.05$; **, $P < 0.001$ versus wild-type cells. Calcium contents are shown as mean ± SEM of six wells. (C) *Runx2* transfectants were treated with anti–IGF-I antibody or LY294002 at the indicated concentrations, and ALP activity (top wells) and mineralization (bottom wells) were examined. ALP activities and calcium contents in two independent clones (#1 and #2) are presented as mean ± SEM of four wells. *, $P < 0.05$; **, $P < 0.001$ versus cells without anti–IGF-I antibody and LY294002 treatment. (D) *Runx2* stable transfectants were infected with EGFP- or dn-*Akt*-expressing adenovirus, and ALP activity (top wells) and mineralization (bottom wells) were examined. ALP activities and calcium contents in two independent Runx2 stable clones (Rinx2#1 and Runx2#2) are presented as mean ± SEM of four wells. *, $P < 0.001$ versus EGFP-expressing adenovirus-infected cells. (E) Wild-type cells (wt) and *Runx2* stable transfectants (*Runx2*) of C3H10T1/2 cells were infected with EGFP- or dn-*Akt*–expressing adenovirus, and ALP activity was examined. ALP activities in wild-type and two independent Runx2 stable clones (Rinx2#1 and Runx2#2) are presented as mean ± SEM of four wells. *, $P < 0.001$ versus EGFP-expressing adenovirus-infected wild-type cells. #, $P < 0.001$ versus EGFP-expressing adenovirus infected Runx2 stable clone. In each experiment, similar results were obtained using at least three independent stable clones.

PI3K-Akt signaling is involved in Runx2-dependent chondrocyte differentiation

We investigated whether or not PI3K-Akt signaling is involved in Runx2-dependent chondrocyte differentiation using ATDC5 cells. ATDC5 cells express *Col1a1* until the cells reach confluence. After confluence, ATDC5 cells condensate and show chondrogenic characteristics including proteoglycan synthesis and *Col2a1* expression in the presence of insulin (Shukunami et al., 1996). Further, ATDC5 cells mature to hypertrophic chondrocytes, which express *Col10a1* (Enomoto et al., 2000). Adenoviral introduction of *Runx2* promoted proteoglycan synthesis and *Col2a1* expression and then *Col10a1* expression, whereas treatment with LY294002 completely prevented proteoglycan production and *Col2a1* and *Col10a1* expression in *Runx2*-overexpressing cells (Fig. 3). Further, adenoviral introduction of dn-*Akt* attenuated the Runx2-enhanced proteoglycan production and *Col2a1* and *Col10a1* expression (Fig. 3). These findings indicate that PI3K-Akt signaling is involved in Runx2-induced chondrocyte differentiation of ATDC5 cells.

Runx2 controls cell migration through PI3K-Akt signaling

When PI3K-Akt signaling was inhibited, Runx2-dependent osteoblast and chondrocyte differentiation were abol-

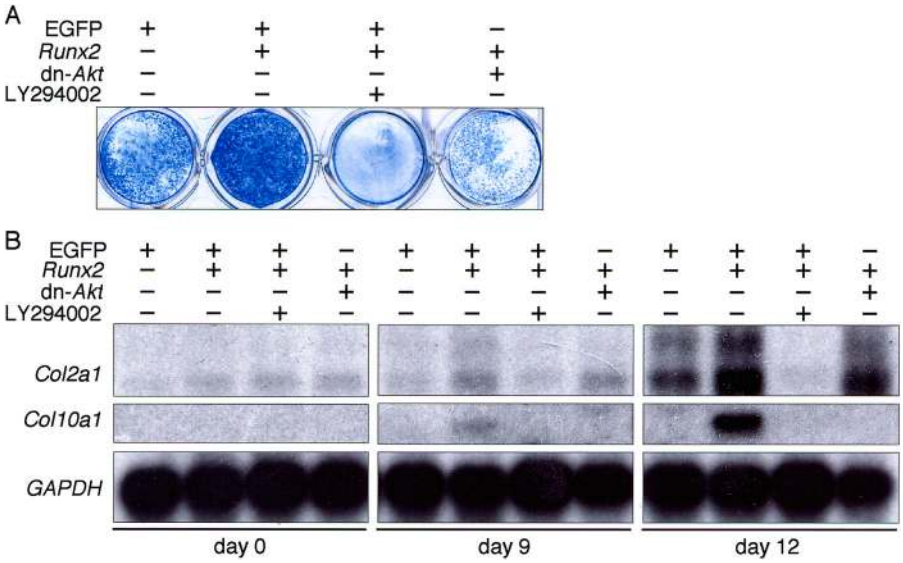

Figure 3. **Blockage of PI3K-Akt signaling inhibits Runx2-dependent chondrogenic differentiation of ATDC5 cells.** (A) Alcian blue staining. (B) Northern blot analysis of *Col2a1* and *Col10a1* mRNA expression. ATDC5 cells were infected with EGFP-expressing adenovirus (EGFP), both EGFP- and *Runx2*-and-EGFP (*Runx2*)–expressing adenoviruses, or both *Runx2*-and-EGFP– and dn-*Akt* (dn-*Akt*)–expressing adenoviruses. After infection, the cells were cultured for 8 d with or without 20 μM LY294002 and stained with Alcian blue (A). In other cells, after infection, RNA was extracted on the indicated days of culture with or without 20 μM LY294002, and *Col2a1* and *Col10a1* expression were examined by Northern blot analysis (B). *GAPDH* was used as an internal control. Similar results were obtained in three independent experiments and representative data are shown.

ished. Therefore, we examined cell migration, which is controlled by PI3K-Akt signaling, in chemotaxis assays using *Runx2* or dn-*Runx2* stable transfectants from MC3T3-E1 cells. Random migration was enhanced in the *Runx2* stable transfectants both in the absence or presence of a chemotactic factor, PDGF, compared with that in wild-type MC3T3-E1 cells, whereas it was suppressed in the dn-*Runx2* stable transfectants, indicating that Runx2 enhances cell motility (Fig. 4, A and B). Further, PDGF-induced chemotaxis was enhanced in the *Runx2* stable transfectants compared with that in the wild-type cells, whereas it was suppressed in the dn-*Runx2* stable transfectants. Similar results were obtained using *Runx2* or dn-*Runx2* stable transfectants from C3T10T1/2 cells and ATDC5

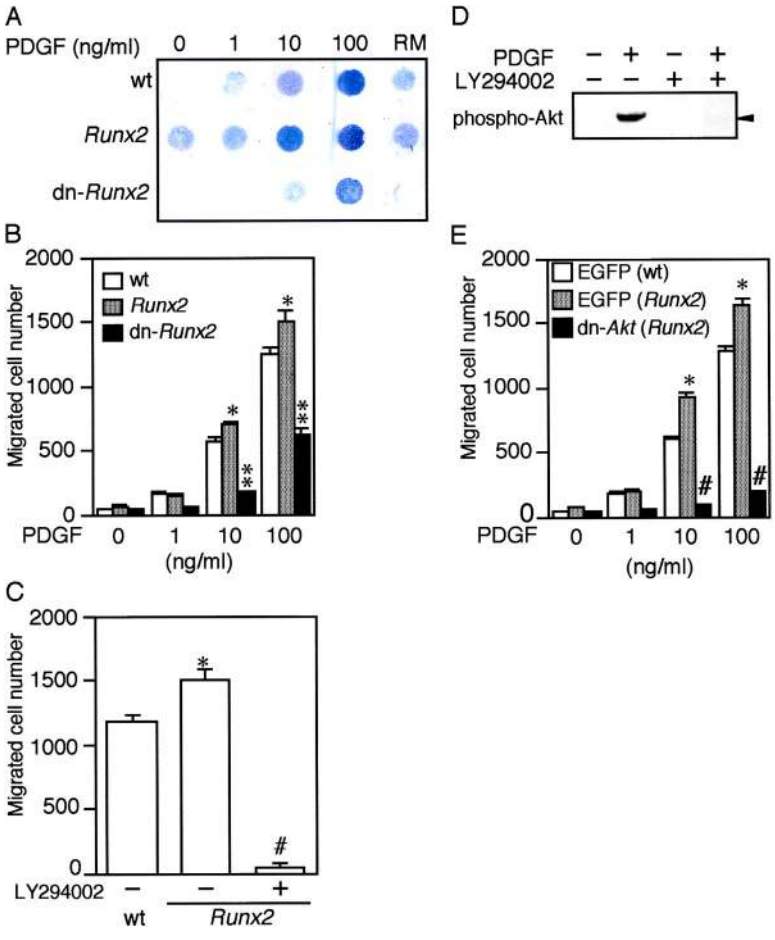

Figure 4. **Runx2 controls cell migration.** Wild-type MC3T3-E1 cells and *Runx2* or dn-*Runx2* stably transfected MC3T3-E1 cells were cultured in the Boyden chamber in the absence or presence of the indicated concentrations of PDGF, and chemotaxis was evaluated as described in Materials and methods. Photograph of the assay filter (A) and the number of cells that migrated to the lower side of the filter (B, Migrated cell number). PDGF was added in the lower wells of the Boyden chamber, except in the random migration experiments in which 100 ng/ml PDGF was added in both the upper and lower wells. Data are presented as mean ± SEM of four wells. *, $P < 0.05$; **, $P < 0.005$ versus wild-type cells at the respective concentration. (C) 100 ng/ml PDGF was added in the lower wells of the Boyden chamber, and wild-type (wt) and *Runx2* stably transfected (*Runx2*) MC3T3-E1 cells were cultured in the absence or presence of 10 μM LY294002. Data are presented as mean ± SEM of four wells. *, $P < 0.05$ versus wild-type cells. #, $P < 0.005$ versus *Runx2* stable transfectants without LY294002 treatment. (D) Wild-type MC3T3-E1 cells were cultured in α-MEM containing 0.1% FCS for 48 h, and then the cells were cultured in the absence or presence of 10 μM LY294002 for 30 min before the addition of PDGF. 50 μg of lysates from cells that had or had not been treated with 100 ng/ml PDGF for 30 min was examined by Western blot analysis using anti-phospho-Akt antibody. (E) Wild-type MC3T3-E1 cells (wt) and *Runx2* stably transfected MC3T3-E1 cells (*Runx2*) were infected with EGFP- or dn-*Akt*–expressing adenovirus. Data are presented as mean ± SEM of four wells. *, $P < 0.01$ versus the respective wild-type cells. #, $P < 0.005$ versus the respective *Runx2* stable transfectants infected with EGFP-expressing adenovirus. In B, C, and E, four separate experiments using independent stable clones were performed and representative data are shown.

cells (unpublished data). Treatment with LY294002 completely abolished the PDGF-induced chemotaxis of *Runx2* stable transfectants (Fig. 4 C). Indeed, PDGF induced phosphorylation of Akt in wild-type MC3T3-E1, C3T10T1/2, and ATDC5 cells, which were inhibited by treatment with LY294002 (Fig. 4 D and not depicted). Adenoviral introduction of dn-*Akt* into *Runx2* stable transfectants abolished the enhancement of chemotaxis induced by Runx2 in the cell migration assay (Fig. 4 E). Similar results were also obtained using MC3T3-E1 cells infected with *Runx2*-expressing adenovirus (unpublished data). These findings indicate that Runx2 enhances cell migration through PI3K-Akt signaling.

Runx2 up-regulates PI3K and Akt protein levels

To investigate whether or not Runx2 affects PI3K-Akt signaling, we examined the expression levels of the PI3K subunits, p85 and p110, and Akt in *Runx2* or dn-*Runx2* stably transfected cells by Western blot analysis (Fig. 5). Overexpression of *Runx2* up-regulated the levels of p85, p110β, and Akt in C3H10T1/2, MC3T3-E1, and ATDC5 cells. Further, phosphorylated Akt was increased in parallel with the level of total Akt protein. In contrast, overexpression of dn-*Runx2* down-regulated the levels of p85, p110β, and Akt proteins in MC3T3-E1 cells and ATDC5 cells. There were no differences in the levels of p110α and p110δ proteins among the wild-type cells, *Runx2* stable transfectants and dn-*Runx2* stable transfectants in the C3H10T1/2 cells, MC3T3-E1 cells, and ATDC5 cells. p110γ was up-regulated only in the *Runx2* stably transfected MC3T3-E1 cells compared with the respective wild-type cells. These findings indicate that Runx2 positively regulates PI3K-Akt signaling by up-regulating the p85, p110β, and Akt protein levels in immature mesenchymal cells, immature osteoblastic cells, and prechondrogenic cells.

We next examined if up-regulation of p85, p110β, and Akt protein levels was due to the transcriptional regulation by RT-PCR analysis. Overexpression of *Runx2* up-regulated mRNA for *p110*β in C3H10T1/2, MC3T3-E1, and ATDC5 cells, whereas overexpression of dn-*Runx2* down-regulated mRNA for *p110*β in MC3T3-E1 and ATDC5 cells. mRNAs for *p85*β, *Akt1*, *Akt2*, and *Akt3* were also mildly up-regulated by overexpression of *Runx2*, but mRNAs for *p85*β, *Akt1*, *Akt2* were subtly down-regulated by overexpression of dn-*Runx2*. In *p85*α, there was no transcriptional regulation by *Runx2*. Therefore, these findings indicate that p110β is mainly regulated by Runx2 at transcriptional level, whereas p85 and Akt are regulated by Runx2 at both transcriptional and protein levels.

As the levels of p85, p110β, and Akt proteins were up-regulated by Runx2, their expression patterns in tibial growth plates were examined in wild-type mouse embryos at E16.5 by immunohistochemistry. The p85, p110β, and Akt protein levels were up-regulated at the stage of prehypertrophic chondrocytes, which express *Pthr1*, and the up-regulation was maintained in hypertrophic chondrocytes, which express *Col10a1* (Fig. 6). The Runx2 protein level was also up-regulated at the stage of prehypertrophic chondrocytes (Fig. 6; Inada et al., 1999; Kim et al., 1999; Enomoto et al., 2000). Therefore, we also examined p85, p110β, and Akt expression in the tibial growth plates of dn-*Runx2* transgenic embryos under the control of the *Col2a1* promoter (Ueta et al., 2001) at E18.5. Up-regulation of p85, p110β, and Akt protein levels was not ob-

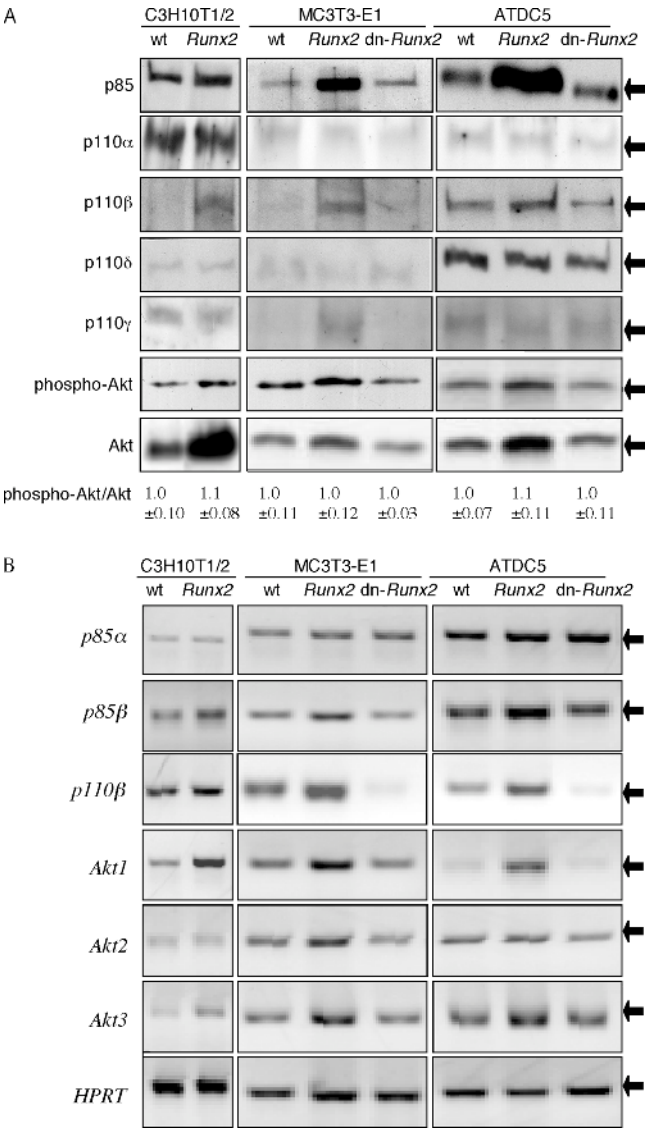

Figure 5. **Western blot and RT-PCR analyses of PI3K subunits (p85 and p110) and Akt.** (A) The expression of p85, p110α, p110β, p110δ, p110γ, phosphorylated Akt (phospho-Akt), and Akt proteins was compared among wild-type (wt) and *Runx2* or dn-*Runx2* stably transfected cells of C3H10T1/2, MC3T3-E1, or ATDC5 cells by Western blot analysis. 20 μg of lysates was loaded. The ratios of phosphorylated Akt versus total Akt are shown in the bottom. The ratio of phosphorylated Akt versus total Akt in wild-type cells of each cell line was defined as one, and relative values are shown. Data are presented as mean ± SEM of three independent experiments. In each cell line, similar results were obtained using three independent stable clones. Arrows show the bands for the indicated proteins. White lines indicate that intervening lanes have been spliced out. (B) The expression of *p85*α, *p85*β, *p110*β, *Akt1*, *Akt2*, and *Akt3* mRNA was compared among wild-type (wt) and *Runx2* or dn-*Runx2* stably transfected cells of C3H10T1/2, MC3T3-E1, or ATDC5 cells by RT-PCR analysis. *HPRT* was used as an internal control. In each cell line, similar results were obtained using three independent stable clones.

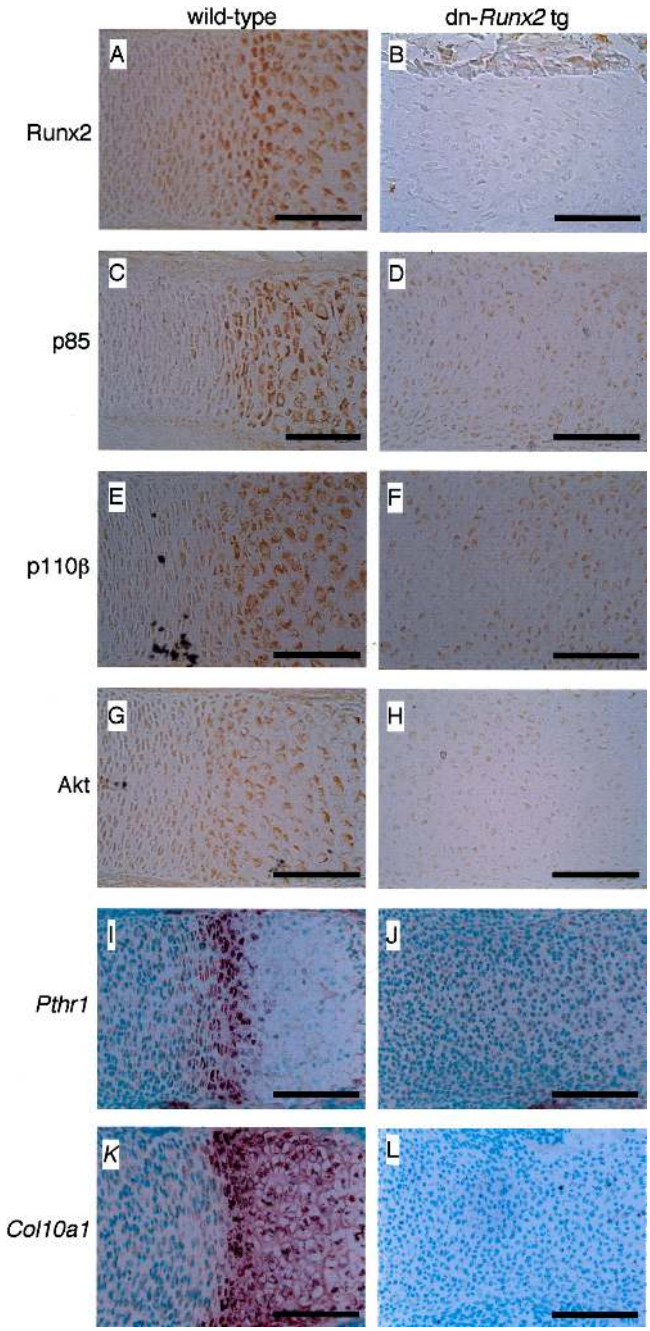

Figure 6. **Runx2, PI3K subunits, and Akt expression in tibial growth plates.** The expression patterns of Runx2 (A and B), p85 (C and D), p110β (E and F), and Akt (G and H) in tibial growth plates from wild-type mice at E16.5 (A, C, E, and G) and dn-*Runx2* transgenic (dn-*Runx2* tg) mice under the control of *Col2a1* promoter at E18.5 (B, D, F, and H) were examined by immunohistochemistry using anti-Runx2, anti-p85, anti-p110β, and anti-Akt antibodies. To clarify the differentiation stage of chondrocytes, the expression of *Pthr1* (I and J) and *Col10a1* (K and L) in tibial growth plates from wild-type mice at E16.5 (I and K) and dn-*Runx2* transgenic mice at E18.5 (J and L) was examined by in situ hybridization using antisense probes of *Pthr1* and *Col10a1*. We detected no signal using the sense probes of *Pthr1* and *Col10a1* (not depicted). Bars, 100 μm.

served in dn-*Runx*2 transgenic embryos, suggesting that Runx2 is involved in the regulation of p85, p110β, and Akt expression in growth plates.

PI3K-Akt signaling enhances DNA binding of Runx2 and Runx2-dependent transcription

We found that treatment of *Runx2* stable transfectants from C3H10T1/2 cells with U0126, a MEK inhibitor, or LY294002 inhibited ALP activity in a dose-dependent manner (Fig. 7 A). To investigate how PI3K-Akt signaling is involved in the activity of Runx2, we examined the effects of LY294002 on the DNA binding of Runx2 and Runx2-dependent transcription, and compared them with the effects of U0126. On electrophoretic mobility shift assay (EMSA) using OSE2 oligonucleotides that contain a Runx binding site, nuclear extracts from *Runx2* stable transfectants of C3H10T1/2 cells formed specific Runx2-Cbfb-DNA complexes (Fig. 7 B). However, treatment of the *Runx2* stable transfectants with LY294002 for 30 min drastically reduced the DNA-binding capacity of Runx2 to less than one-tenth (Fig. 7, B and C). In contrast, treatment of the cells with U0126 for 30 min had no effect on the DNA-binding capacity of Runx2 (Fig. 7 B), although prolonged treatment for 24 h gradually reduced the DNA binding of Runx2 up to one-fourth (Fig. 7 C). Treatment with LY294002 or U0126 did not affect the level of Runx2 protein in the *Runx2* stable transfectants (Fig. 7 B). In reporter assays using the osteocalcin promoter, treatment with either LY294002 or U0126 for 48 h severely reduced the level of Runx2-dependent transcription in *Runx2* stable transfectants from C3H10T1/2 cells (Fig. 7 D). Further, chromatin immunoprecipitation assays showed that treatment with LY294002 prevented the binding of Runx2 to endogenous osteocalcin promoter in wild-type MC3T3-E1 cells (Fig. 7 E). These findings indicate that the DNA-binding capacity of Runx2 and transcriptional activation by Runx2 are dependent on the activities of both PI3K and MEK, but the mechanisms through which PI3K and MEK regulate Runx2 function are quite different.

As the treatment with anti–IGF-I antibody severely inhibited osteoblastic differentiation of MC3T3-E1 cells (Fig. 2 C), we further examined the effect of the treatment with anti–IGF-I antibody in the DNA binding of Runx2. The DNA binding of Runx2 was diminished by the treatment with anti–IGF-I antibody (Fig. 7 F). However, overexpression of *Runx2* failed to induce *Igf1* (Fig. 7 G). These findings indicate that Runx2 is not involved in *Igf1* induction, but IGF-I signaling plays an important role in Runx2-dependent osteoblastic differentiation of MC3T3-E1 cells.

Next, we examined the DNA binding of Runx2 and Runx2-dependent transcription in myr*Akt* and dn-*Akt* stable transfectants. DNA binding of Runx2 was strongly enhanced in myr*Akt* stable transfectants of MC3T3-E1 cells compared with that in wild-type MC3T3-E1 cells (Fig. 8 A). In reporter assays using the osteocalcin promoter, Runx2-dependent transcription was strongly enhanced in the myr*Akt* stable transfectants, but was absent in dn-*Akt* stable transfectants of MC3T3-E1 cells (Fig. 8 B). However, overexpression of myr*Akt* or dn-Akt did not affect the protein levels of Runx2 or Cbfb (Fig. 8 C). Adenoviral introduction of dn-*Akt* in *Runx2* stable transfectants of C3H10T1/2 cells severely reduced the DNA binding of Runx2 (Fig. 8 D). In reporter assays using the osteocalcin promoter, introduction of dn-*Akt* in *Runx2* stable trans-

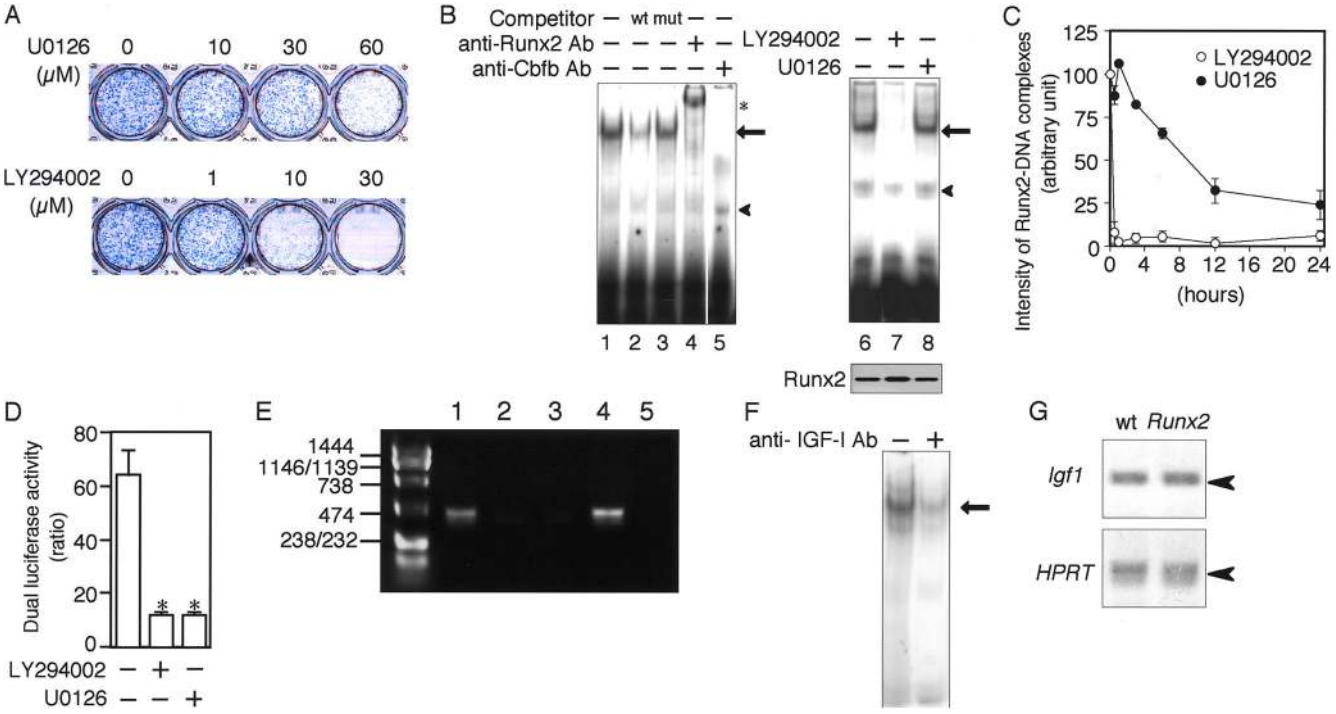

Figure 7. **Inhibitors of PI3K and MEK inhibit DNA binding of Runx2 and Runx2-dependent transcription.** (A) After confluence, *Runx2* transfectants were treated with U0126 or LY294002 at the indicated concentrations for 3 d and ALP activity was examined. Three separate experiments using independent stable clones were performed and representative data are shown. (B) On EMSA using OSE2 oligonucleotides, nuclear extract from *Runx2* stably transfected C3T10T1/2 cells showed a specific band (arrows), which was competitively bound by unlabeled OSE2 oligonucleotides (lane 2, 100-fold molar excess), but not by mutated oligonucleotides (lane 3, 100-fold molar excess). Addition of antibody against Runx2 supershifted the specific band (lane 4), and addition of antibody against Cbfb prevented formation of the specific Runx2-Cbfb-DNA complexes (lane 5). Treatment with 10 μM LY294002 for 30 min, but not with 20 μM U0126 for 30 min, prevented the formation of the specific Runx2-Cbfb-DNA complexes (lanes 7 and 8). Asterisk indicates the supershifted complexes, and arrowheads indicate nonspecific bands. The level of Runx2 protein was examined in the nuclear extracts of lanes 6–8 by Western blot analysis (bottom panel). White line indicates that an intervening lane has been spliced out. (C) DNA-binding activity of Runx2 was examined at the indicated times after the addition of 10 μM LY294002 or 20 μM U0126 to the cell cultures. The intensity of Runx2-DNA complexes in *Runx2* stably transfected C3H10T1/2 cells before LY294002 or U0126 treatment was defined as 100, and the relative intensities are shown. The data are presented as mean ± SEM of four independent experiments. Three separate experiments were performed, and they showed similar results. (D) Reporter assays using the osteocalcin promoter. *Runx2* stably transfected C3H10T1/2 cells were transiently transfected with p147mOG2/luciferase reporter construct (p147-luc). After culture for 24 h, the medium was replaced with medium containing 2% FCS and the transfected cells were cultured without or with 10 μM LY294002 or 20 μM U0126 for 48 h. Data are presented as mean ± SEM of four wells. *, $P < 0.005$ versus cells without LY294002 and U0126 treatment. Four separate experiments using independent stable clones were performed, and representative data are shown. (E) Chromatin immunoprecipitation assay. After the culture for 3 d in medium containing ascorbic acid, MC3T3-E1 cells were cultured with or without 10 μM LY294002 for 30 min, and samples were prepared as described in Materials and methods. After chromatin immunoprecipitation by anti-Runx2 antibody, purified DNAs from immunoprecipitates without Ly294002 treatment (lane1), immunoprecipitates with LY294002 treatment (lane 2), supernatants without LY294002 treatment (lane 3), and supernatants with LY294002 treatment (lane 4) were amplified by PCR using the primers in the mouse osteocalcin promoter region. Chromatin immunoprecipitation was also performed using anti-HA antibody as a negative control, and no specific band was amplified using purified DNA from immunoprecipitates without Ly294002 treatment (lane 5). (F) Runx2 stable transfectants of MC3T3-E1 cells were treated with 80 μg/ml IGF-I antibody for 3 d, and EMSA was performed using OES2 oligonucleotides. (G) RT-PCR analysis of *Igf1* expression. After confluence, wild-type and *Runx2* stably transfected MC-3T3-E1 cells were cultured for 3 d in the presence of ascorbic acid, and mRNAs were isolated for RT-PCR. *HPRT* was used as an internal control.

fectants of C3H10T1/2 cells dose dependently inhibited Runx2-dependent transcription, which was similar to the effect of dn-*Runx2* (Fig. 8 E). These findings indicate that PI3K-Akt signaling plays an important role in the DNA binding of Runx2 and transcriptional activation by Runx2.

We further examined whether or not Akt is involved in the phosphorylation of Runx2 by immunoprecipitation assays using anti-Runx2 antibody in myr*Akt*-transfected ATDC5 cells. The phosphorylation levels of tyrosine, serine, and threonine in Runx2 were similar between wild-type and myr*Akt*-transfected ATDC5 cells (Fig. 8 F). Further, a similar level of Runx2 was detected in wild-type and myr*Akt*-transfected ATDC5 cells in the immunoprecipitation assays using antiphosphotyrosine, antiphosphoserine, or antiphosphothreonine antibody (unpublished data). These findings suggest that phosphorylation of Runx2 is not a major mechanism for the activation of Runx2 by Akt.

Discussion

We showed that PI3K-Akt signaling is deeply involved in Runx2-dependent osteoblast and chondrocyte differentiation and their migration. Runx2 enhanced PI3K-Akt signaling by up-regulating the protein levels of PI3K subunits and

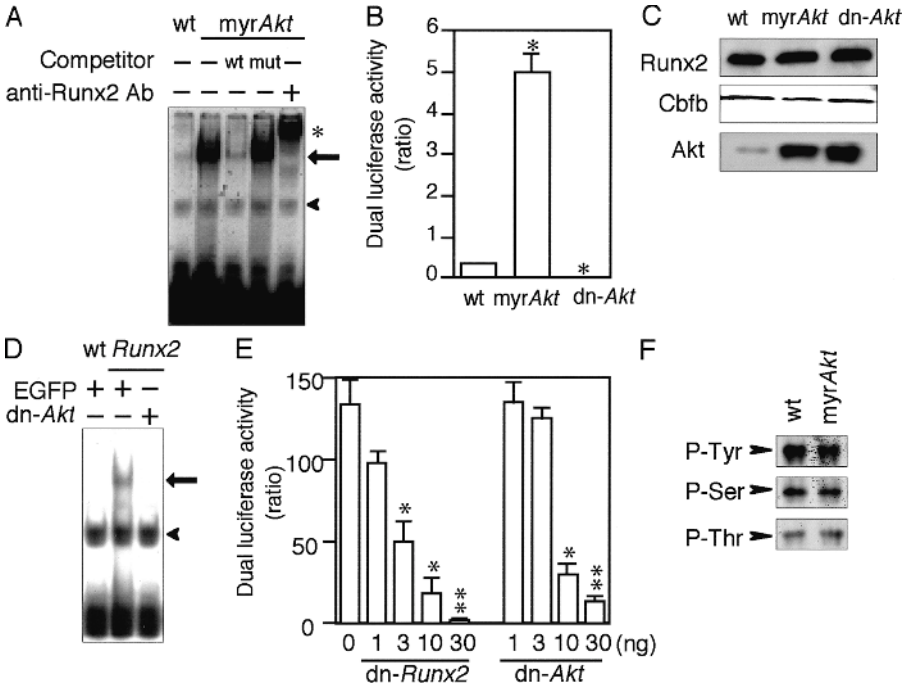

Figure 8. **Akt regulates DNA binding of Runx2 and Runx2-dependent transcription.** (A) EMSA using cell lysates from wild-type and myr*Akt* stably transfected MC3T3-E1 cells. The intensity of the specific band (arrow) was greatly enhanced in myr*Akt* stably transfected MC3T3-E1 cells. The specific band was competitively bound by unlabeled OSE2 oligonucleotides (wt, 100-fold molar excess), but not by mutated OSE2 oligonucleotides (mut, 100-fold molar excess). The addition of Runx2 antibody supershifted the specific band (asterisk). Arrowhead indicates nonspecific bands. (B) Reporter assays using the osteocalcin promoter. Wild-type MC3T3-E1 cells and myr*Akt* or dn-*Akt* stably transfected MC3T3-E1 cells were transiently transfected with p147-luc. Data are presented as mean ± SEM of four wells. *, $P < 0.05$ versus wild-type cells. (C) Western blot analysis. Nuclear extracts and whole-cell lysates were prepared from wild-type MC3T3-E1 cells and myr*Akt* or dn-*Akt* stably transfected MC3T3-E1 cells. 10 μg of nuclear extracts was loaded and the filter was hybridized with anti-Runx2 antibody. 20 μg of whole-cell lysates was loaded and the filters were hybridized with anti-Cbfb antibody or anti-Akt antibody. (D) Wild-type cells (wt) and *Runx2* stable transfectants (*Runx2*) of C3H10T1/2 cells were infected with EGFP- or dn-*Akt*-expressing adenovirus. EMSA was performed using OSE2 oligonucleotides. The introduction of dn-*Akt* inhibited the formation of Runx2-DNA complexes (arrow). Arrowhead indicates nonspecific bands. (E) The indicated amounts of dn-*Runx2* or dn-*Akt* construct were transiently cotransfected with p147-luc in *Runx2* stably transfected C3H10T1/2 cells. Data are presented as mean ± SEM of four wells. *, $P < 0.05$; **, $P < 0.005$ versus cells without transfection of dn-*Runx2* and dn-*Akt*. In each experimental condition, four separate experiments using independent stable clones were performed and representative data are shown. (F) The level of phosphorylation of Runx2. Nuclear extracts from wild-type and myr*Akt* stable transfected ATDC5 cells at confluence were immunoprecipitated using anti-Runx2 antibody, and the immunoprecipitates were transferred to nylon membranes and reacted with antiphosphotyrosine, antiphosphoserine, or antiphosphothreonine antibody. Four independent experiments showed similar results, and representative data are shown.

Akt, whereas PI3K-Akt signaling greatly enhanced DNA binding of Runx2 and Runx2-dependent transcription. This positive feedback loop further augments Runx2 activity in osteoblast and chondrocyte differentiation and their migration. Thus, our findings indicate that Runx2 and PI3K-Akt signaling are mutually dependent on each other in the regulation of osteoblast and chondrocyte differentiation and their migration.

Treatment with LY294002 or introduction of dn-*Akt* severely inhibited Runx2-induced osteoblastic and chondrogenic differentiation of C3H10T1/2, MC3T3-E1, and ATDC5 cells (Figs. 2 and 3), indicating that PI3K-Akt signaling is involved in Runx2 functioning at multiple steps of osteoblast differentiation as well as chondrocyte differentiation. MAPK-dependent phosphorylation of Runx2 stimulates Runx2-dependent transcription (Xiao et al., 2000), and protein kinase A phosphorylates the transactivation domain of Runx2 (Selvamurugan et al., 2000). In contrast, Runx2 is negatively regulated by serine phosphorylation (Wee et al., 2002). Treatment with LY294002 for 30 min severely diminished DNA binding of Runx2 without affecting the levels of both Runx2 and Cbfb proteins (Fig. 7), but the phosphorylation levels of tyrosine, serine, and threonine in Runx2 were not affected by the overexpression of myr*Akt* (Fig. 8 F). Although a possibility that Akt modulates phosphorylation of Runx2 cannot be excluded, it is possible that PI3K-Akt signaling regulates the DNA-binding activity of Runx2 by phosphorylation of some molecules that form a DNA-binding complex with Runx2 or their dephosphorylation through the activation of phosphatase, because interactions with other transcription factors such as Ets, Smads, and C/EBP, with the transcription cofactor Rb, and with the transcriptional repressor TLE greatly influence the activity of Runx2 (Komori, 2002). However, the mechanism of the phosphorylation or dephosphorylation of DNA-binding complex molecules containing Runx2 by PI3K-Akt signaling should be different from that by the MAPK pathway because the time courses of the inhibition of the DNA-binding activity of Runx2 were quite different between the treatments with LY294002 and U0126 (Fig. 7 C).

In accordance with our findings, bone development in *Igf1*/*Igf2* mutant mice, *Igf1r* mutant mice, and *Akt1*/*Akt2* mutant mice is severely delayed (Liu et al., 1993, Peng et al., 2003). However, the delay in bone development in these mutant mice is still milder than that in *Runx2*$^{-/-}$ mice (Komori et al., 1997, Otto et al., 1997), suggesting that stimulation with other ligands such as VEGF in addition to IGFs may also be involved in the activation of PI3K-Akt signaling, and that Akt3 in addition to Akt1 and Akt2 may function in osteoblast and chondrocyte differentiation. However, in the case of MC3T3-E1 cells it is likely that IGF-I is a major ligand for the activation of PI3K-Akt signaling and Runx2 function and

that autocrine stimulation by IGF-I is important for differentiation because treatment with anti–IGF-I antibody severely inhibited the osteoblastic differentiation induced by Runx2 and DNA binding of Runx2 (Fig. 2 C and Fig. 7 F).

In growth plates, proliferating chondrocytes begin to mature to prehypertrophic chondrocytes and further mature to hypertrophic chondrocytes. In this maturation process, the Runx2, p85, p110β, and Akt protein levels were all up-regulated at the stage of prehypertrophic chondrocytes, and the up-regulation was maintained during the hypertrophic stage (Fig. 6). Further, Runx2 up-regulated the p85, p110β, and Akt protein levels (Fig. 5), and PI3K-Akt signaling activated Runx2 function (Figs. 7 and 8). Therefore, the positive feedback loop of Runx2 and PI3K-Akt signaling is likely to play important roles in the maturational process of chondrocytes at the growth plates.

We showed that Runx2 is involved in cell migration. Runx2 increased chemotaxis of C3H10T1/2, MC3T3-E1, and ATDC5 cells, and it was abrogated by treatment with LY294002 or the introduction of dn-*Akt* (Fig. 4 and not depicted), indicating that Runx2 induces cell migration through PI3K-Akt signaling. However, as IGF-I has no significant effect on the cell migration of MC3T3-E1 cells (Fukuyama et al., 2004), activation of another signaling pathway in addition to PI3K-Akt signaling pathway may be required for the cell migration, and Runx2 may be involved in the activation of both signaling pathways. The significance of chemotaxis in bone and cartilage formation has not been shown. However, as *Runx2* is expressed in the precursors of osteoblasts and chondrocytes (Ducy et al., 1997, Otto et al., 1997), Runx2 may play a role in the migration of these precursors to the appropriate sites during skeletal development. Runx2 may also play a role in bone remodeling by inducing the migration of osteoblasts to the surface of bone that has undergone osteolysis by osteoclasts. As *Runx2* expression is strongly induced in osteoblastic cells after bone fracture (Kawahata et al., 2003), chemotaxis enhanced by Runx2 should be important for the migration of osteoblastic cells to the healing area. Indeed, after a bone fracture, the positive feedback loop of Runx2 and PI3K-Akt signaling would play important roles in multiple healing processes including the migration of chondrogenic and osteoblastic cells and their precursors to the healing place, chondrocyte maturation that leads to the replacement of cartilage with bone, and osteoblast differentiation.

We showed the linkage of Runx2 and the PI3K-Akt signaling pathway in osteoblast and chondrocyte differentiation and their migration. However, PI3K-Akt signaling is involved in multiple cell functions including cell proliferation, apoptosis, cell growth, and glucose metabolism in addition to cell differentiation and migration. Therefore, the cell phenotypes resulting from the coupling of Runx2 and PI3K-Akt signaling may be more complex, and they need to be further investigated.

Materials and methods

Cell cultures

C3H10T1/2 and ATDC5 cells were purchased from RIKEN Cell Bank. MC3T3-E1 subclone 4 was a gift from R.T. Franceschi (University of Michigan School of Dentistry, Ann Arbor, MI; Xiao et al., 2000). C3H10T1/2 cells were cultured in BME and MC3T3-E1 cells were cultured in α-MEM containing 10% FBS (GIBCO BRL). ATDC5 cells were cultured as previously described (Enomoto et al., 2000). Cells were treated with anti–IGF-I antibody (Upstate Biotechnology), LY294002 (Calbiochem), or U0126 (Calbiochem). The percentages of dead cells, which were less than 3% by a trypan blue exclusion assay, were not significantly different among all of the experiments.

Establishment of stably transfected cells

To generate a dn-*Runx2*-expressing vector, a 421-bp DNA fragment containing the runt domain of *Runx2* was subcloned into pSG5 (Stratagene). The vectors, myr*Akt*, which has the c-Src myristoylation sequence fused in frame to the NH_2 terminus of the *Akt* coding sequence, and dn-*Akt* [T308A, S473A], were gifts from K. Walsh (St. Elizabeth's Medical Center, Boston, MA; Fujio et al., 1999). The day before transfection, cells were plated on 35-mm dishes at a density of 10^5 cells per milliliter. *Runx2*-expressing vector (Harada et al., 1999), dn-*Runx2*-expressing vector, myr*Akt*-expressing vector, or dn-*Akt*-expressing vector was transfected using FuGENE 6 (Roche). A vector containing the neomycin-resistant gene and the respective vector were cotransfected in the cells. Cells were grown to subconfluence, trypsinized, plated at low density, and selected in the presence of 400 μg/ml G418 for 3 wk. Colonies were isolated by digestion with trypsin/EDTA for 5 min at 37°C within stainless steel cloning rings. Four to five independent clones were established in each expression vector.

Adenoviral transfer

Bicistronic adenovirus vectors expressing type II *Runx2* and EGFP or EGFP alone were generated as previously described (Yoshida et al., 2002). Dn-*Akt*–expressing adenovirus was a gift from K. Walsh (Fujio et al., 1999). Cells were plated at a density of 2×10^4 cells per well in 24-well plates. They were infected with EGFP-expressing, *Runx2*-and-EGFP–expressing, and/or dn-*Akt*–expressing adenoviruses at a multiplicity of infection of 10 or 20 for 12 or 24 h.

Cytochemical and immunohistochemical examinations and in situ hybridization

Detection and quantification of ALP activity, von Kossa staining, Alizarin red staining, and calcium quantification were performed as described previously (Enomoto et al., 2000; Kobayashi et al., 2000). Dn-*Runx2* transgenic mice were generated as previously described (Ueta et al., 2001). Immunohistochemical analysis was performed using rabbit anti-p85 (Upstate Biotechnology), rabbit anti-p110β (Santa Cruz Biotechnology, Inc.), rabbit anti-Akt (New England Biolabs, Inc.), or mouse monoclonal anti-Runx2 (Yoshida et al., 2002) antibody as described previously (Liu et al., 2001). In situ hybridization was performed using a 0.8-kb fragment of mouse *Pthr1* cDNA and a 0.65-kb fragment of mouse *Col10a1* cDNA for probes as previously described (Ueta et al., 2001). Sections were counterstained with methyl green. The images were acquired by Axioskop 2 Plus (Carl Zeiss MicroImaging, Inc.) with an objective lens (PlanNeofluar, 40×/0.75) and AxioCam HRc (Carl Zeiss MicroImaging, Inc.) using AxioVision 3.0 at 22°C. The images were processed in size and brightness using Adobe Photoshop 5.5. Before the study, all experiments were reviewed and approved by Osaka University Medical School Animal Care and Use Committee.

Northern blot and RT-PCR

Northern blot was performed using a 0.4-kb fragment of mouse *Col2a1* cDNA, a 0.65-kb fragment of mouse *Col10a1* cDNA, and a 0.85-kb fragment of mouse *GAPDH* cDNA, as described previously (Inada et al., 1999). For RT-PCR, cDNA (10 ng total RNA equivalent) was amplified by Amp Taq DNA polymerase (PerkinElmer) using the following primers: *p85*α, 5′-ATTTCACCCCCTACTCCCAA-3′ and 5′-GGCTGTCTCTCATTCCATTC-3′; *p85*β, 5′-CGCAACACGGACAGACTGGT-3′ and 5′-TAGCAGCAGCACAGGGAAGT-3′; *p110*β, 5′-CTGTGACCCCGCAGAAAAAT-3′ and 5′-CATACTCCACTCTCCCACTG-3′; *Akt1*, 5′-CGTAGCCATTGTGAAGGAGG-3′ and 5′-CCCTTGCCCAGTAGTTTCAG-3′; *Akt2*, 5′-GTCGCCAACAGTCTGAAGCA-3′ and 5′-GAGAGAGGTGGAAAAACAGC-3′; *Akt3*, 5′-AAGGTTGGGTTCAGAAGAGG-3′ and 5′-CTGTGAGGTTGGGCTACAAT-3′; *hypoxanthin guanine phosphoribosyl transferase* (*HPRT*), 5′-GCTGGTGAAAAGGACCTCT-3′ and 5′-CACAGGACTAGAACAACTGC-3′; *Igf1*, 5′-GCTCTGCTTGCTCACCTTCA-3′ and 5′-CGATAGGGACGGGGACTTCT-3′. 25 cycles (*p85*α), 20 cycles (*p85*β, *p110*β, *Akt1*, *Akt2*, *Akt3*, and *Igf1*), and 15 cycles (*HPRT*) of amplification were performed using a Gene Amp PCR system 2400 (PerkinElmer; 30 s at 94°C, 30 s at 64°C, and 1 min at 72°C). Amplified products were verified by subcloning and sequence analysis. PCR products were transferred to nylon membranes and hybridized with the respective ^{32}P-labeled probes.

Western blot and immunoprecipitation analyses

Western blot analyses were performed using nuclear extracts or whole cell lysates as described previously (Yoshida et al., 2002). The blots were first incubated with rabbit anti-p85 antibody, which recognizes both p85α and p85β (Upstate Biotechnology); rabbit anti-p110α antibody; rabbit anti-p110β antibody; rabbit anti-p110δ antibody; rabbit anti-p110γ antibody (Santa Cruz Biotechnology, Inc.); rabbit anti-Akt antibody, which recognizes Akt1, Akt2, and Akt3 (New England Biolabs, Inc.); rabbit anti-phospho-Akt antibody (New England Biolabs, Inc.); goat anti-Runx2 antibody (Santa Cruz Biotechnology, Inc.); or monoclonal Cbfb antibody (a gift from Y. Ito, Institute of Molecular and Cell Biology, Singapore; Yoshida et al., 2002); and then with HRP-conjugated anti–rabbit or anti–mouse IgG (New England Biolabs, Inc.) or anti–goat IgG (Santa Cruz Biotechnology, Inc.). Immunoprecipitation was performed using Seize™X protein G immunoprecipitation kit (Pierce Chemical Co.) to avoid contamination of IgG band according to the manufacturer's protocol using nuclear extract samples, anti-Runx2 antibody (Santa Cruz Biotechnology, Inc.), and antiphosphotyrosine, antiphosphoserine, and antiphosphothreonine mAbs (Seikagaku Corp.).

Cell migration assay

Cell migration assays were performed using PDGF-BB (PeproTech) as described previously (Fukuyama et al., 2004). Cells were placed in the upper wells at 10^5 cells per well. After culture for 12 h, the filters were removed, fixed in 100% methanol, and stained with Diff-Quick (International Reagent Corp.). The top side of the filter was then scraped free of cells with a cotton swab. The number of cells that migrated to the bottom side was counted manually.

EMSA

Nuclear extracts were prepared, and EMSA was performed as described previously (Yoshida et al., 2002). Competition was performed with either a 100-fold molar excess of unlabeled OSE2 oligonucleotides or a 100-fold molar excess of mutated oligonucleotides. For supershift experiments, mAb against Runx2 or Cbfb (gifts from Y. Ito; Yoshida et al., 2002) was added to the entire mixture. Protein–DNA complexes were resolved on 6% nondenaturing polyacrylamide gels.

Reporter assay

Reporter assays were performed by transient transfection of 0.2 μg of p147mOG2/Luciferase reporter construct (p147-luc) and 0.002 μg of pRL-CMV using Dual Luciferase Reporter Assay System (Promega) as described previously (Yoshida et al., 2002). Luciferase activity was measured using a model TD20/20 luminometer (Promega) and normalized to *Renilla* luciferase activity under the control of CMV promoter.

Chromatin immunoprecipitation assay

Chromatin immunoprecipitation was performed as described previously (Yoshida et al., 2004). After immunoprecipitation using anti-Runx2 antibody (Santa Cruz Biotechnology, Inc.), DNAs were purified from the supernatants and immunoprecipitates, respectively. PCR was performed using the following primers in the promoter region (−471/−67) of the mouse *osteocalcin* gene: CTGAACTGGGCAAATGAGGACA and AGGGGATGCTGCCAGGACTAAT.

Statistical analysis

Statistical analyses were performed using *t* test. $P < 0.05$ was considered to be significant.

We thank R.T. Franceschi for the MC3T3-E1 cells, K. Walsh for the myr*Akt* and dn-*Akt* vectors, Y. Ito for the Runx2 and Cbfb antibody, T. Furuichi and N. Kanatani for helpful discussion, R. Hiraiwa for maintaining mouse colonies, and M. Yanagita for secretarial assistance.

This work was supported by grants from the Ministry of Education, Science and Culture of Japan (T. Fujita, Y. Azuma, and T. Komori) and by the Sasakawa Scientific Research Grant from The Japan Science Society (T. Fujita).

Submitted: 28 January 2004
Accepted: 4 May 2004

References

Akiyama, H., T. Kanno, H. Ito, A. Terry, J. Neil, Y. Ito, and T. Nakamura. 1999. Positive and negative regulation of chondrogenesis by splice variants of PEBP2αA/CBFα1 in clonal mouse EC cells, ATDC5. *J. Cell. Physiol.* 181: 169–178.

Akune, T., N. Ogata, K. Hoshi, N. Kubota, Y. Terauchi, K. Tobe, H. Takagi, Y. Azuma, T. Kadowaki, K. Nakamura, et al. 2002. Insulin receptor substrate-2 maintains predominance of anabolic function over catabolic function of osteoblasts. *J. Cell Biol.* 159:147–156.

Banerjee, C., L.R. McCabe, J. Choi, S.W. Hiebert, J.L. Stein, G.S. Stein, and J.B. Lian. 1997. Runt homology domain proteins in osteoblast differentiation: AML3/CBFA1 is a major component of a bone-specific complex. *J. Cell. Biochem.* 66:1–8.

Bi, W., J.M. Deng, Z. Zhang, R.R. Behringer, and B. de Crombrugghe. 1999. Sox9 is required for cartilage formation. *Nat. Genet.* 22:85–89.

Ducy, P., R. Zhang, V. Geoffroy, A.L. Ridall, and G. Karsenty. 1997. Osf2/Cbfa1: a transcriptional activator of osteoblast differentiation. *Cell.* 89:747–754.

Enomoto, H., M. Enomoto-Iwamoto, M. Iwamoto, S. Nomura, M. Himeno, Y. Kitamura, T. Kishimoto, and T. Komori. 2000. Cbfa1 is a positive regulatory factor in chondrocyte maturation. *J. Biol. Chem.* 275:8695–8702.

Fujio, Y., K. Guo, T. Mano, Y. Mitsuuchi, J.R. Testa, and K. Walsh. 1999. Cell cycle withdrawal promotes myogenic induction of Akt, a positive modulator of myocyte survival. *Mol. Cell. Biol.* 19:5073–5082.

Fukuyama, R., T. Fujita, Y. Azuma, T. Hirano, H. Nakamuta, M. Koida, and T. Komori. 2004. Statins inhibit osteoblast migration by inhibiting Rac-Akt signaling. *Biochem. Biophys. Res. Commun.* 315:636–642.

Ghosh-Choudhury, N., S.L. Abboud, R. Nishimura, A. Celeste, L. Mahimainathan, and G.G. Choudhury. 2002. Requirement of BMP-2-induced phosphatidylinositol 3-kinase and Akt serine/threonine kinase in osteoblast differentiation and Smad-dependent BMP-2 gene transcription. *J. Biol. Chem.* 277:33361–33368.

Harada, H., S. Tagashira, M. Fujiwara, S. Ogawa, T. Katsumata, A. Yamaguchi, T. Komori, and M. Nakatsuka. 1999. Cbfa1 isoforms exert functional differences in osteoblast differentiation. *J. Biol. Chem.* 274:6972–6978.

Hidaka, K., T. Kanematsu, H. Takeuchi, M. Nakata, U. Kikkawa, and M. Hirata. 2001. Involvement of the phosphoinositide 3-kinase/protein kinase B signaling pathway in insulin/IGF-I-induced chondrogenesis of the mouse embryonal carcinoma-derived cell line ATDC5. *Int. J. Biochem. Cell Biol.* 33:1094–1103.

Huang, B.K., L.A. Golden, G. Tarjan, L.D. Madison, and P.H. Stern. 2000. Insulin-like growth factor I production is essential for anabolic effects of thyroid hormone in osteoblasts. *J. Bone Miner. Res.* 15:188–197.

Inada, M., T. Yasui, S. Nomura, S. Miyake, K. Deguchi, M. Himeno, M. Sato, H. Yamagiwa, T. Kimura, N. Yasui, et al. 1999. Maturational disturbance of chondrocytes in Cbfa1-deficient mice. *Dev. Dyn.* 214:279–290.

Kaliman, P., F. Vinals, X. Testar, M. Palacin, and A. Zorzano. 1996. Phosphatidylinositol 3-kinase inhibitors block differentiation of skeletal muscle cells. *J. Biol. Chem.* 271:19146–19151.

Karaplis, A.C. 2002. Embryonic development of bone and the molecular regulation of intramembranous and endochondral bone formation. *In* Principles of Bone Biology. J.P. Bilezikian, L.G. Raisz, and G.A. Rodan, editors. Academic Press, London. 33–58.

Kawahata, H., T. Kikkawa, Y. Higashibata, T. Sakuma, M. Huening, M. Sato, M. Sugimoto, K. Kuriyama, K. Terai, Y. Kitamura, et al. 2003. Enhanced expression of Runx2/PEBP2alphaA/CBFA1/AML3 during fracture healing. *J. Orthop. Sci.* 8:102–108.

Kim, I.S., F. Otto, B. Zabel, and S. Mundlos. 1999. Regulation of chondrocyte differentiation by cbfa1. *Mech. Dev.* 80:159–170.

Kobayashi, H., Y. Gao, C. Ueta, A. Yamaguchi, and T. Komori. 2000. Multilineage differentiation of Cbfa1-deficient calvarial cells in vitro. *Biochem. Biophys. Res. Commun.* 273:630–636.

Komori, T. 2002. Runx2, a multifunctional transcription factor in skeletal development. *J. Cell. Biochem.* 87:1–8.

Komori, T., H. Yagi, S. Nomura, A. Yamaguchi, K. Sasaki, K. Deguchi, Y. Shimizu, R.T. Bronson, Y.H. Gao, M. Inada, et al. 1997. Targeted disruption of Cbfa1 results in a complete lack of bone formation owing to maturational arrest of osteoblasts. *Cell.* 89:755–764.

Liu, J.P., J. Baker, A.S. Perkins, E.J. Robertson, and A. Efstratiadis. 1993. Mice carrying null mutations of the genes encoding insulin-like growth factor I (Igf-1) and type 1 IGF receptor (Igf1r). *Cell.* 75:59–72.

Liu, W., S. Toyosawa, T. Furuichi, N. Kanatani, C. Yoshida, Y. Liu, M. Himeno, S. Narai, A. Yamaguchi, and T. Komori. 2001. Overexpression of Cbfa1 in osteoblasts inhibits osteoblast maturation and causes osteopenia with multiple fractures. *J. Cell Biol.* 155:157–166.

Nakashima, K., X. Zhou, G. Kunkel, Z. Zhang, J.M. Deng, R.R. Behringer, and

B. de Crombrugghe. 2002. The novel zinc finger-containing transcription factor osterix is required for osteoblast differentiation and bone formation. *Cell.* 108:17–29.

Ogata, N., D. Chikazu, N. Kubota, Y. Terauchi, K. Tobe, Y. Azuma, T. Ohta, T. Kadowaki, K. Nakamura, and H. Kawaguchi. 2000. Insulin receptor substrate-1 in osteoblast is indispensable for maintaining bone turnover. *J. Clin. Invest.* 105:935–943.

Otto, F., A.P. Thornell, T. Crompton, A. Denzel, K.C. Gilmour, I.R. Rosewell, G.W. Stamp, R.S. Beddington, S. Mundlos, B.R. Olsen, et al. 1997. Cbfa1, a candidate gene for cleidocranial dysplasia syndrome, is essential for osteoblast differentiation and bone development. *Cell.* 89:765–771.

Peng, X.D., P.Z. Xu, M.L. Chen, A. Hahn-Windgassen, J. Skeen, J. Jacobs, D. Sundararajan, W.S. Chen, S.E. Crawford, K.G. Coleman, et al. 2003. Dwarfism, impaired skin development, skeletal muscle atrophy, delayed bone development, and impeded adipogenesis in mice lacking Akt1 and Akt2. *Genes Dev.* 17:1352–1365.

Ridley, A.J., M.A. Schwartz, K. Burridge, R.A. Firtel, M.H. Ginsberg, G. Borisy, J.T. Parsons, and A.R. Horwitz. 2003. Cell migration: integrating signals from front to back. *Science.* 302:1704–1709.

Sakaue, H., W. Ogawa, M. Matsumoto, S. Kuroda, M. Takata, T. Sugimoto, B.M. Spiegelman, and M. Kasuga. 1998. Posttranscriptional control of adipocyte differentiation through activation of phosphoinositide 3-kinase. *J. Biol. Chem.* 273:28945–28952.

Scheid, M.P., and J.R. Woodgett. 2001. PKB/AKT: functional insights from genetic models. *Nat. Rev. Mol. Cell Biol.* 2:760–768.

Selvamurugan, N., M.R. Pulumati, D.R. Tyson, and N.C. Partridge. 2000. Parathyroid hormone regulation of the rat collagenase-3 promoter by protein kinase A-dependent transactivation of core binding factor alpha1. *J. Biol. Chem.* 275:5037–5042.

Shukunami, C., C. Shigeno, T. Atsumi, K. Ishizeki, F. Suzuki, and Y. Hiraki. 1996. Chondrogenic differentiation of clonal mouse embryonic cell line ATDC5 in vitro: differentiation-dependent gene expression of parathyroid hormone (PTH)/PTH-related peptide receptor. *J. Cell Biol.* 133:457–468.

Smits, P., P. Li, J. Mandel, Z. Zhang, J.M. Deng, R.R. Behringer, B. de Croumbrugghe, and V. Lefebvre. 2001. The transcription factors L-Sox5 and Sox6 are essential for cartilage formation. *Dev. Cell.* 1:277–290.

Ueta, C., M. Iwamoto, N. Kanatani, C. Yoshida, Y. Liu, M. Enomoto-Iwamoto, T. Ohmori, H. Enomoto, K. Nakata, K. Takada, et al. 2001. Skeletal malformations caused by overexpression of Cbfa1 or its dominant negative form in chondrocytes. *J. Cell Biol.* 153:87–99.

Wee, H.J., G. Huang, K. Shigesada, and Y. Ito. 2002. Serine phosphorylation of RUNX2 with novel potential functions as negative regulatory mechanisms. *EMBO Rep.* 3:967–974.

Xiao, G., D. Jiang, P. Thomas, M.D. Benson, K. Guan, G. Karsenty, and R.T. Franceschi. 2000. MAPK pathways activate and phosphorylate the osteoblast-specific transcription factor, Cbfa1. *J. Biol. Chem.* 275:4453–4459.

Yoshida, C.A., T. Furuichi, T. Fujita, R. Fukuyama, N. Kanatani, S. Kobayashi, M. Satake, K. Takada, and T. Komori. 2002. Core-binding factor beta interacts with Runx2 and is required for skeletal development. *Nat. Genet.* 32: 633–638.

Yoshida, C.A., H. Yamamoto, T. Fujita, T. Furuichi, K. Ito, K. Inoue, K. Yamana, A. Zanma, K. Takada, Y. Ito, and T. Komori. 2004. Runx2 and Runx3 are essential for chondrocyte maturation and Runx2 regulates limb growth through induction of Indian hedgehog. *Genes Dev.* 18:952–963.